University of Tehran Press

Online ISSN: 2345-475X

DESERT

Home page: https://jdesert.ut.ac.ir/

Drought Mapping in the Southern Zagros Mountains Using ERA5-Land Reanalysis Data and the Standardized Precipitation-Evapotranspiration Index

Zahra Javi[1], Hossein Madadi[1*], Hamid Taleshi[1], Reza Shakeri[1]

[1] Department of Environmental Sciences and Engineering, Faculty of Natural Resources, Behbahan Khatam Al-anbia University of Technology, Behbahan, Iran. Email: madadi@bkatu.ac.ir

Article Info.

Article type:
Research Article

Article history:
Received: 14 Feb. 2025
Received in revised from: 01 Apr. 2026
Accepted: 02 May 2026
Published online: 18 May 2026

Keywords:
SPEI,
ERA5-Land,
Zagros,
Climate change,
Hydrological drought,
Trend analysis.

ABSTRACT

Drought poses significant threats to water security in mountainous regions, particularly under climate warming. This study maps drought dynamics in the Southern Zagros Mountains (Iran) using ERA5-Land reanalysis data downscaled to 1 km resolution via the TopoPyScale framework, integrating topographic corrections for precipitation, temperature, and potential evapotranspiration (PET). The Standardized Precipitation-Evapotranspiration Index (SPEI) was computed at 3-, 6-, and 12-month timescales to assess meteorological, agricultural, and hydrological droughts from 2000 to 2022. Results reveal strong elevational gradients, with mean annual precipitation ranging from <200 mm yr^{-1} in southeastern lowlands to >800 mm yr^{-1} along northwestern ridges, and PET declining from >1500 mm yr^{-1} to <1200 mm yr^{-1} with altitude. Spatiotemporal patterns indicate recurrent mild to moderate summer droughts at short timescales, escalating into severe multi-year events (2008–2012, 2018–2021) affecting >60% of the area. Drought frequency is highest (0.45–0.58 events/year) in lowlands, while durations extend to 13–17 months in snow-dependent highlands. Trend analysis shows significant negative SPEI shifts across 45–50% of the region, with slopes of -0.025 to -0.040 per year, driven by warming and increased PET. These findings highlight topography's role in modulating drought vulnerability, offering insights for enhanced water management and climate adaptation in southwestern Iran. The approach demonstrates the value of downscaled reanalysis for precise drought monitoring in complex terrains.

Cite this article: Javi, Z., Madadi, H., Taleshi, H., Shakeri, R. (2026). A Drought Mapping in the Southern Zagros Mountains Using ERA5-Land-Land Reanalysis Data and the Standardized Precipitation-Evapotranspiration Index. DESERT, 30 (2), DOI: 10.22059/jdesert.2025.107088

DOI: 10.22059/jdesert.2025.107088

Publisher: University of Tehran Press

1. Introduction

Drought represents a complex; multifaceted natural hazard rooted in sustained imbalances within the hydrological cycle. Its manifestations encompass a range of impacts, including meteorological, agricultural, hydrological, and socio-ecological consequences (Disasa *et al*., 2025). Meteorologically, drought is typically characterized by a prolonged deficit in precipitation compared to established climatological norms. This phenomenon is frequently quantified using standardized indices, notably the Standardized Precipitation Index (SPI) and the Standardized Precipitation–Evapotranspiration Index (SPEI) (Dai, 2011; Vicente-Serrano *et al*., 2010). Furthermore, hydrological drought emerges as precipitation deficits propagate through the terrestrial water cycle, leading to reduced streamflow, diminished reservoir storage, and impaired groundwater recharge (Van Loon, 2015). Simultaneously, agricultural drought is triggered by soil moisture depletion and heightened atmospheric evaporative demand, ultimately restricting crop yields and pasture availability (Vicente-Serrano *et al*., 2013). Given the ongoing effects of climate warming, the frequency, duration, and severity of drought events are escalating in numerous regions globally. These intensified conditions pose significant challenges to food security, ecological stability, and socio-economic development, as highlighted by the Intergovernmental Panel on Climate Change (IPCC, 2021; Dai, 2013).

Mountain environments are fundamentally important to regional and continental water resources, acting as significant reservoirs for precipitation in the form of seasonal snow and ice. Subsequently, meltwater is released, contributing to downstream basin hydrology (Liu *et al*., 2021). However, these environments are notably vulnerable to hydro-climatic extremes due to a confluence of factors including steep topographic gradients, shallow soils, fractured bedrock, and the pronounced influence of orographic processes on precipitation and temperature. This combination results in rapid runoff, limited groundwater recharge, and considerable spatial variability in water availability (Viviroli *et al*., 2011; Shah *et al*., 2014). Furthermore, alterations in snow accumulation and accelerated glacier retreat exacerbate drought vulnerability by dynamically modulating both the magnitude and seasonality of streamflow (Barnett *et al*., 2005; Shen *et al*., 2013). Consequently, the impacts of drought in mountain regions frequently propagate rapidly across a range of ecological and human systems, including biodiversity, rangelands, irrigated agriculture, and urban water supplies.

Monitoring drought conditions in mountainous regions presents a significant challenge due to the limitations of traditional observation networks (Yuan and Liao, 2025). Existing station data are frequently sparse and characterized by coarse-resolution climate products, which often fail to adequately represent the substantial influence of elevation, slope, and aspect on both precipitation and temperature patterns. While widely utilized drought indices, including the Standardized Precipitation Index (SPI), Standardized Precipitation-Evaporation Index (SPEI), and Palmer Drought Severity Index (PDSI), offer valuable diagnostic insights, they can be inadequate in capturing localized variability intrinsically linked to complex topographic features and snow processes (Shen *et al*., 2013; Vicente-Serrano *et al*., 2013). Recent advancements in reanalysis products and topographic downscaling techniques offer promising solutions. These approaches leverage the integration of physically consistent atmospheric data with high-resolution terrain information, thereby facilitating a more nuanced understanding of drought dynamics within these challenging environments (Fiddes & Gruber, 2014; De Grandchamp & Favier, 2011).

The ERA5-Land reanalysis dataset, produced by the European Centre for Medium-Range Weather Forecasts (ECMWF), constitutes a significant advancement in the availability of long-

term, spatially consistent climate data, offering valuable resources for drought analysis. Providing hourly atmospheric and land-surface variables from 1979 to the present at a nominal spatial resolution of 0.1°, ERA5-Land has become widely adopted within hydro-climatic and drought research (Muñoz-Sabater *et al*., 2021). Despite these improvements in resolution and physical consistency, the dataset may exhibit underestimation of local extremes and snow-related processes, particularly within complex terrain, necessitating downscaling and terrain-aware corrections to ensure reliable drought assessments (Land *et al*., 2023).

Among available drought indicators, the SPEI has emerged as a robust, multiscalar index that explicitly incorporates both precipitation supply and atmospheric evaporative demand (Vicente-Serrano *et al*., 2010). This formulation is particularly advantageous for drought assessment under climate-warming conditions, demonstrating superior performance compared to precipitation-only indices, especially within agricultural and hydrological applications (Beguería *et al*., 2014; Dai, 2013). The SPEI's multi-timescale nature allows for the characterization of short-term agricultural drought alongside longer-term hydrological and water-resource drought.

The Southern Zagros Mountains, a critical water-producing region within Iran, exhibit heightened vulnerability to drought due to their Mediterranean-type climate, pronounced seasonality, and reliance on snowmelt-dominated runoff. While previous research has documented historical drought variability across the broader Zagros region, spatially explicit assessments integrating high-resolution climate data with topographic corrections remain comparatively limited (Beiranvand *et al*., 2024, Sadrianzadeh *et al*., 2023). Furthermore, projected warming and alterations in precipitation patterns are anticipated to intensify water stress within this region during the coming decades, as highlighted in the IPCC Sixth Assessment Report (IPCC, 2021).

Against the backdrop of increasing environmental vulnerability, this study undertakes a comprehensive spatiotemporal analysis of drought conditions within the Southern Zagros Mountains. Utilizing ERA5-Land reanalysis data in conjunction with topographic downscaling via the TopoPyScale framework and the SPEI, the research seeks to achieve the following objectives. First, high-resolution precipitation and temperature fields were generated across the complex topography of the region. Second, multi-timescale SPEI values were calculated to rigorously characterize drought frequency, severity, and persistence. Finally, long-term trends in drought conditions were identified using non-parametric statistical techniques. These findings offer novel insights into the dynamics of drought within this climatically sensitive mountain system and, consequently, contribute to enhanced water-resource management and climate adaptation planning initiatives in southwestern Iran.

2. Materials and methods

2.1. Study Area

The study area encompasses the structurally complex Southern Zagros Mountains within the Zagros Fold-and-Thrust Belt of southwestern Iran (26.9° to 31.9° N and 49.7° to 57.1° E). Topography within this region exhibits a significant gradient, ranging from approximately 0 meters at the southeastern periphery to exceeding 4405 meters along the prominent northwestern ridges. The area is characterized by a Mediterranean climate, distinguished by cool, wet winters and hot, dry summers. Precipitation, predominantly concentrated between November and April, is strongly influenced by orographic lifting, resulting in marked spatial variations in both temperature and precipitation, and consequently, localized microclimates.

Notably, substantial snow accumulation at higher elevations, followed by seasonal melt, represents a critical source of surface runoff and groundwater recharge. This reliance on seasonal water storage makes the region particularly vulnerable to the impacts of interannual climate variability and protracted drought conditions.

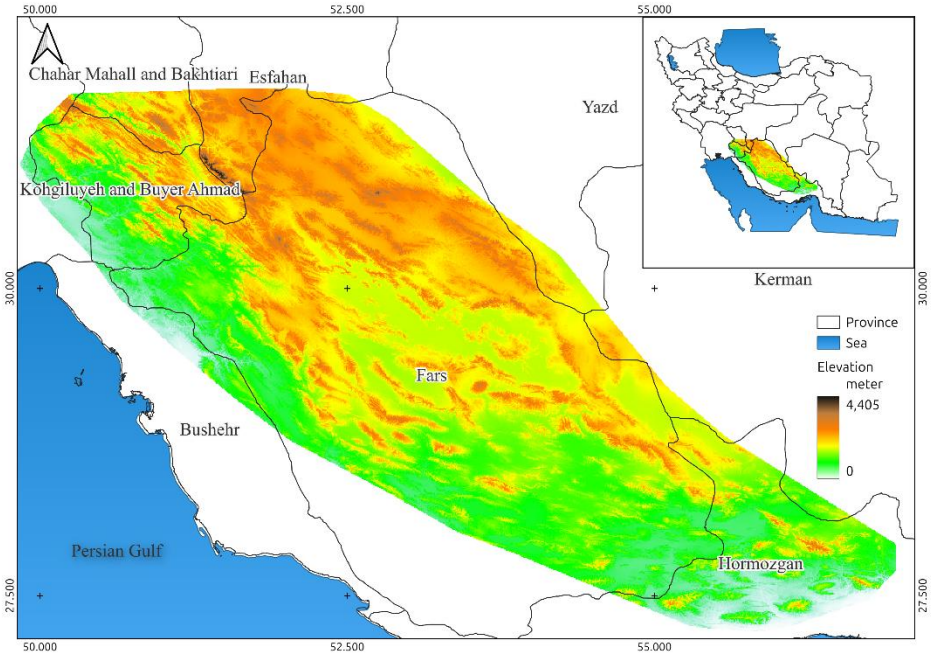

Figure 1. Elevation map and delineated boundary of the Southern Zagros Mountains study area.

2.2. Data Sources

Monthly precipitation and 2-meter air temperature data were acquired from the ERA5-Land reanalysis dataset (Muñoz-Sabater *et al*., 2021), provided by the European Centre for Medium-Range Weather Forecasts (ECMWF). The ERA5-Land dataset offers globally consistent atmospheric and land surface variables, characterized by a spatial resolution of 0.1° and has undergone rigorous validation for applications in hydro-climatology. To facilitate topographic downscaling of climate variables, a digital elevation model (DEM) with a spatial resolution of 1 km was employed to represent terrain characteristics. This approach acknowledges the crucial role of topography in influencing regional climate patterns.

2.3. Topographic Downscaling

To improve the spatial resolution of climate variables across complex topography, daily ERA5-Land precipitation and temperature fields were subjected to downscaling using the TopoPyScale framework (Fiddes & Gruber, 2014). This approach, predicated on a physically based statistical–dynamical methodology, effectively redistributed the coarse-resolution reanalysis data by incorporating elevation, slope, aspect, and atmospheric lapse rates. Specifically, temperature fields were corrected via the application of elevation-dependent lapse rates, while precipitation adjustments were achieved through the utilization of orographic scaling factors derived from the local terrain characteristics. The resultant high-resolution monthly precipitation and temperature datasets subsequently served as the foundation for subsequent drought index calculations.

2.4. Estimation of Reference Evapotranspiration

Monthly reference evapotranspiration (PET) was calculated using the Thornthwaite method, which establishes a relationship between PET and mean air temperature, alongside latitude-dependent day length (Thornthwaite, 1948). While acknowledging its relative simplicity compared to more sophisticated, physically-based formulations, the Thornthwaite method continues to be a prevalent approach within studies utilizing the SPEI – a key factor ensuring methodological alignment with the original SPEI framework (Vicente-Serrano *et al*., 2010). Monthly Heat Index (Thornthwaite) was calculated using the following equations (1 – 4).

$$i_m = \left(\frac{T_m}{5}\right)^{1.514}, T_m > 0 \quad (1)$$

where i_m is monthly heat index, and T_m is mean air temperature of month m(∘C),

$$I = \sum_{m=1}^{12} \Im \quad (2)$$

where I is annual heat index.

$$\alpha = 6.75 \times 10^{-7} I^3 - 7.71 \times 10^{-5} I^2 + 1.792 \times 10^{-2} I + 0.49239 \quad (3)$$

where α is Thornthwaite Exponent.

$$PET = 16 \left(\frac{10T}{I}\right)^{\alpha} \times \frac{L}{12} \times \frac{N}{30} \quad (4)$$

Where:

- L = mean day length (hours)
- N = number of days in month

2.5. SPEI

Drought conditions were quantified using the Standardized Precipitation-Evapotranspiration Index (SPEI) based on the methodology outlined by Vicente-Serrano *et al*. (2010). At each grid cell, a monthly climatic water balance was calculated using the equation (5).

$$D_i = P_i - PET_i \quad (5)$$

where P_i represents monthly precipitation and PET_i denotes monthly reference evapotranspiration. These water-balance series were subsequently aggregated at 3-, 6-, and 12-month timescales to characterize short-term agricultural drought, seasonal hydrological drought, and long-term water-resource drought, respectively. For each aggregation period, a three-parameter log-logistic distribution was applied to the data, and the resulting series were transformed into standardized normal variates to generate SPEI values exhibiting a mean of zero and a variance of one (equations 6-8). The python was utilized for all computational procedures.

Accumulation Over Time Scale *k*, For a time scale k (e.g., 3, 6, 12 months):

$$D_t^{(k)} = \sum_{i=0}^{k-1} D_{t-i} \quad (6)$$

The accumulated water balance series Dt (k) is fitted to a log-logistic distribution:

$$F(x) = \frac{1}{1+\left(\frac{\beta}{x-y}\right)^{\propto}} \quad (7)$$

where:

- α = shape parameter
- β = scale parameter
- γ = location parameter

Parameters are estimated using maximum likelihood estimation (MLE).
The cumulative probability is transformed into a standard normal variable:

$$SPEI_t = \Phi^{-1}\left(F\left(D_t^{(k)}\right)\right) \quad (8)$$

where:

- Φ−1 = inverse standard normal distribution

This ensures:

- Mean = 0
- Standard deviation = 1

Drought severity was then classified as mild (−1.0 ≤ SPEI < −0.5), moderate (−1.5 ≤ SPEI < −1.0), severe (−2.0 ≤ SPEI < −1.5), and extreme (SPEI < −2.0).

2.6. Spatiotemporal Analysis

To examine interannual variability in drought patterns, monthly SPEI grids were aggregated to generate annual means. Subsequently, drought frequency, duration, and mean severity were calculated for each grid cell and timescale. The resulting spatial drought maps facilitated the identification of persistent drought hotspots within the study area. Furthermore, analysis of regional mean SPEI time series allowed for a comprehensive characterization of large-scale drought variability and its temporal dynamics.

2.7. Trend Analysis

Long-term trends in drought conditions were investigated utilizing non-parametric statistical methods designed to mitigate the influence of non-normality and outliers. The Mann–Kendall test (Mann, 1945; Kendall, 1975) was employed to analyze annual SPEI series for each grid cell, with the objective of identifying monotonic trends at a 95% confidence level. Where statistically significant trends were observed, the magnitude of change was determined using Sen's slope estimator (Sen, 1968). To account for potential spatial autocorrelation and the complexities associated with multiple testing, a bootstrap resampling approach was utilized to rigorously assess field significance.

3. Results

3.1. Downscaled Climate Variables

The downscaling of ERA5-Land reanalysis data using TopoPyScale (Fiddes & Gruber, 2014) produced high-resolution (1 km) grids of precipitation (P), temperature (T), and potential evapotranspiration (PET) for the Southern Zagros Mountains from 2000 to 2022, revealing pronounced topographic controls on climate patterns. This section presents the spatiotemporal characteristics of these variables, highlighting orographic enhancements and elevational gradients that underscore the region's vulnerability to drought. Mean annual precipitation exhibited strong spatial heterogeneity, ranging from less than 200 mm in the low-elevation southeastern foothills to over 800 mm yr^{-1} along the high northwestern ridges (Figure 2). This distribution reflects orographic precipitation enhancement, with gradients of 50-100% increase per 1000 m elevation, as windward slopes intercept moist air masses from the Persian Gulf

(Table 1). Compared to raw ERA5-Land data at 0.25° resolution, the downscaled fields captured microclimatic variations, such as localized rainfall shadows in leeward valleys, reducing biases in complex terrain by incorporating elevation-dependent scaling factors.

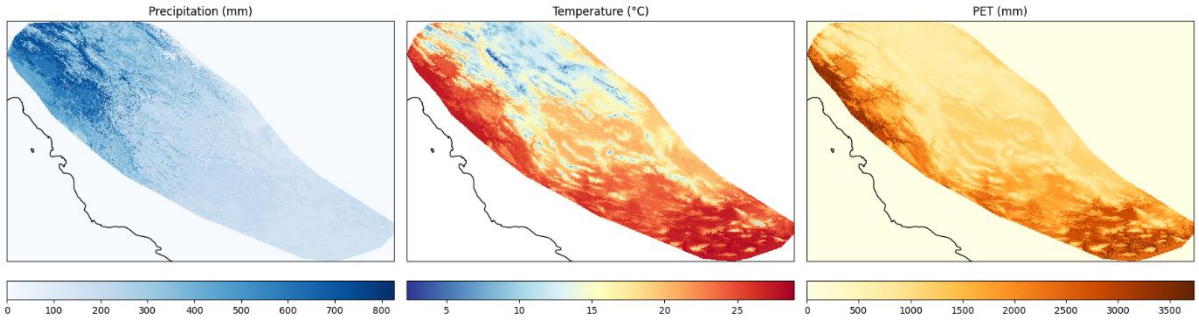

Figure 2. Multi-Panel Maps of Mean Annual P, T, and PET (2000- 2022)

Analysis of temperature data revealed a marked inverse correlation with elevation. Mean annual temperatures demonstrated a consistent decline, decreasing from approximately 25°C in arid lowlands (below 1000 m) to temperatures consistently below 10°C at elevations above 3000 m (Figure 2). This reduction in temperature with increasing altitude is attributable, in part, to the effects of solar radiation attenuation and adiabatic cooling processes, factors commonly associated with mountainous terrain.

Table 1. Summary Statistics by Elevation Bands

Elevation Band	Mean P (mm yr^{-1})	Min P	Max P	Std P	Mean T (°C)	Mean PET (mm yr^{-1})
<1000 m	285.6	141.1	747.9	160.1	26.03	2438.07
1000–2000 m	266.1	72.9	826.3	176.7	20.47	1263.02
2000–3000 m	299.5	72.9	826.3	128.5	13.57	755.06
>3000 m	291.9	130.8	826.3	85.5	7.52	538.26

Analysis of temperature lapse rates indicates a mean decrease of approximately −5 to −7 °C km^{-1}, consistent with adiabatic cooling processes typical of mountainous environments (Figure 3). Trend analysis reveals a warming rate of about 0.2–0.5 °C $decade^{-1}$, with amplification at higher elevations, in agreement with reported climate change signals in Mediterranean-type regions (Shen *et al*., 2013). Potential evapotranspiration (PET), estimated using the Thornthwaite approach (Thornthwaite, 1948; Vicente-Serrano *et al*., 2010), exceeds 1500 mm yr^{-1} in hot, arid lowlands, reflecting enhanced atmospheric demand under elevated temperatures (Figure 2). At higher elevations, PET decreases to below 1200 mm yr^{-1} due to cooler conditions, although an increasing trend of 1–3% per decade persists, likely driven by regional warming (Land *et al*., 2023). These results underscore the strong control of topography on regional water balance. Moreover, the applied downscaling techniques improve spatial detail, yielding climate fields that better capture the heterogeneity of the Southern Zagros and provide a reliable foundation for subsequent SPEI-based drought assessments.

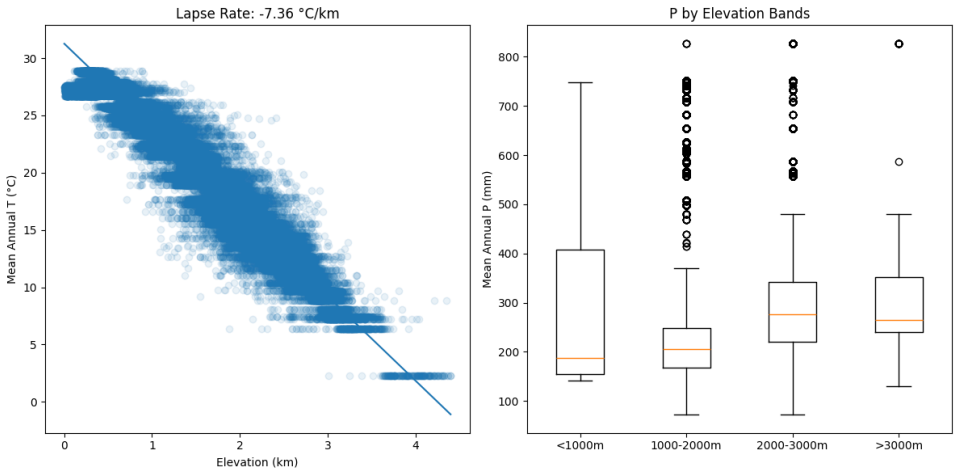

Figure 3. Scatter Plots/Boxplots of P/T vs. Elevation

3.1.1. Validation against in-situ observations

To evaluate the reliability of the downscaled ERA5-Land air temperature used in the SPEI computation, station-based observations from five synoptic stations (Abadeh, Fasa, Gachsaran, Yasoge, and Shiraz Shahid Dastghaib International Airport) were compared against the corresponding downscaled surface temperature values (Figure 4). The comparison reveals an exceptionally strong agreement across all stations, with Pearson correlation coefficients (r) ranging from 0.988 to 0.993, and coefficients of determination (R^2) consistently exceeding 0.97. Root Mean Square Error (RMSE) values remain low, varying between 1.05 °C and 3.41 °C, indicating limited systematic bias and high fidelity of the downscaling procedure. Regression slopes closely follow the 1:1 reference line, particularly at Yasoge and Gachsaran stations, suggesting that both cold and warm temperature extremes are well preserved. Minor dispersion observed at Abadeh and Fasa is primarily associated with seasonal transition periods, which are known to amplify local surface–atmosphere interactions in mountainous and semi-arid environments. Overall, these results confirm that the downscaled ERA5-Land temperature data accurately reproduce observed station-scale thermal variability and are suitable for robust SPEI-based drought assessment across the Southern Zagros region.

Station-based precipitation observations were similarly evaluated against downscaled ERA5-Land precipitation to assess the uncertainty associated with the primary water-balance input to SPEI (Figure 5). In contrast to temperature, precipitation exhibits greater spatial variability and event-scale uncertainty, which is reflected in more heterogeneous performance metrics across stations. Correlation coefficients range from 0.674 (Abadeh) to 0.928 (Yasoge), with corresponding R^2 values between 0.45 and 0.86. Despite this variability, stations located in regions with stronger orographic control (e.g., Yasoge and Shiraz) demonstrate substantially improved agreement, suggesting that downscaling benefits from terrain-driven precipitation signals. Lower performance at Abadeh is primarily attributed to the dominance of convective and sporadic rainfall events, which remain challenging for reanalysis-based products. Nevertheless, the overall correspondence indicates that downscaled ERA5-Land precipitation captures the dominant temporal variability necessary for drought monitoring, particularly when aggregated over monthly to multi-month SPEI time scales.

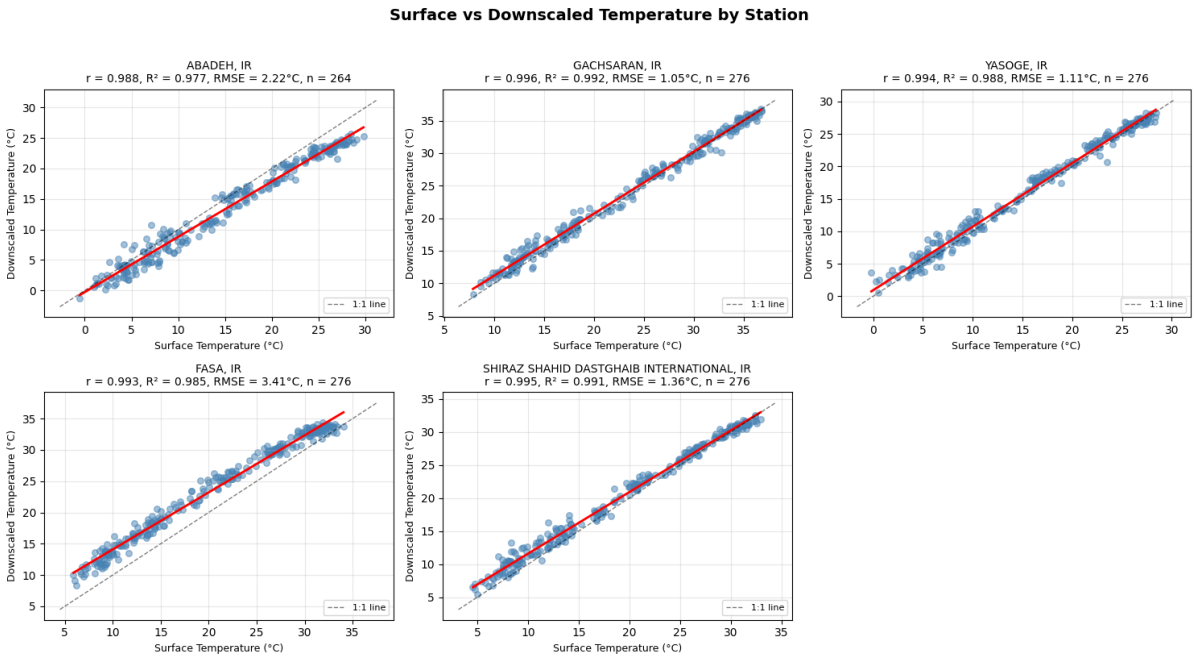

Figure 4. Surface versus downscaled ERA5-Land temperature comparison at selected stations

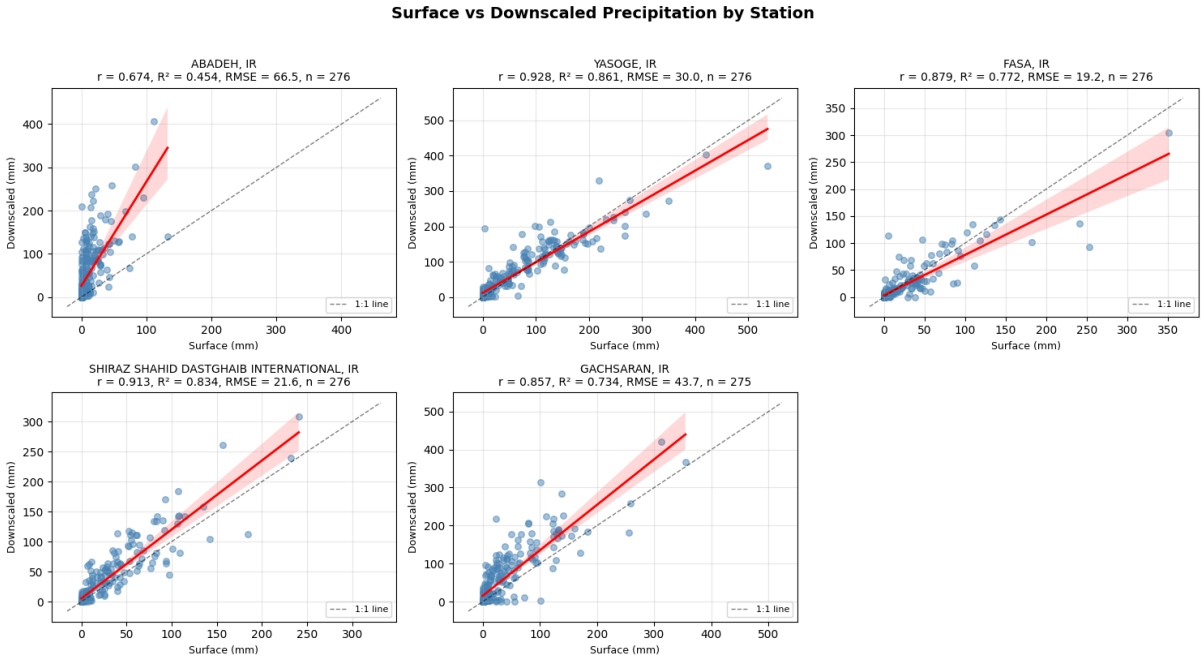

Figure 5. Surface versus downscaled ERA5-Land precipitation comparison at selected stations

3.2. Spatiotemporal Patterns of SPEI

Analysis of SPEI values at 3-, 6-, and 12-month timescales identified discernible patterns of drought variability within the Southern Zagros Mountains between 2000 and 2022. Notably, SPEI-3, designed to capture meteorological and agricultural drought events, demonstrated a

recurrent occurrence of mild to moderate droughts primarily during the summer months, characterized by substantial spatial heterogeneity. Specifically, severe drought conditions, defined by SPEI values below -1.5, were concentrated in the low-elevation southeastern plains, a region where limited snowmelt buffering contributed to amplified moisture deficits. In contrast, the highland areas exhibited comparatively milder conditions. These observations align with the Mediterranean-type climate prevalent in the region, which is characterized by elevated evaporative demand during the summer months (Vicente-Serrano *et al*., 2010; Alijani, 2008).

Table 2. List of major drought events for SPEI-12 (2000-2022).

Event	Start/End Dates	Duration (months)	Mean Severity	% Area Affected
1	2008-01 to 2012-12	60	-1.5	65
2	2018-01 to 2021-12	48	-1.8	72
3	2001-01 to 2002-06	18	-1.2	55

Analysis of SPEI values – SPEI-6 and SPEI-12, which serve as indicators of seasonal and long-term hydrological droughts – revealed a pattern of extended drought events between 2008 and 2012 and again from 2018 to 2021. These periods impacted over 60% of the study area, with extreme SPEI values (SPEI < -2) concentrated within southeastern low-elevation zones (Table 2). These events align with documented regional drought conditions observed in Iran, primarily attributable to decreased winter precipitation and rising temperatures (Lotfirad *et al*., 2021). Examination of regional mean SPEI time series demonstrated a sustained increase in negative values following 2010, characterized by slopes of -0.02 to -0.05 per year. This trend was linked to a roughly 20% reduction in winter precipitation and a corresponding 10% increase in the temperature-potential evapotranspiration (T/PET) ratio (Fig. 6). Drought hotspots were delineated, with northwestern high ridges exhibiting fewer, yet more severe, drought occurrences (mean severity of approximately -1.5, with durations of 12-18 months for SPEI-12), likely due to their reliance on snowmelt. Conversely, the southeastern plains demonstrated a higher frequency of drought events (0.5-0.7 events per year), a consequence of limited snow storage capacity and elevated PET levels. Ultimately, the multi-timescale SPEI data underscored the progression of meteorological droughts into significant hydrological impacts, with approximately 50% of the area experiencing severe or extreme conditions during major drought episodes.

3.3. Drought Frequency, Duration, and Severity

Analysis of drought characteristics within the Southern Zagros Mountains revealed substantial topographic influences on drought frequency, duration, and severity, assessed at a grid cell level and subsequently aggregated by elevation and regional sub-divisions (2000-2022). Drought events were operationalized as consecutive months exhibiting SPEI values below -0.5 for general drought assessments (mild and worse) and below -1.5 for severe and extreme cases, aligning with established classifications (Vicente-Serrano *et al*., 2010; Beguería *et al*., 2014). Frequency was quantified as the number of events per effective year (calculated as time series length divided by 12 months), duration was defined as the average length of events in months, and severity was represented by the mean SPEI value during event periods (McKee *et al*., 1993).

Specifically, SPEI-3 analysis indicated the highest drought frequency (0.45-0.58 events yr^{-1}) in the low-elevation southeastern plains, which subsequently decreased to <0.18 in the high-

elevation northwestern zones (Table 3; Figure 7).

This spatial pattern is attributable to limited snowpack retention and elevated evaporative demand within the lowland regions, thereby intensifying short-term agricultural droughts (Vicente-Serrano *et al*., 2013). The average duration of SPEI-3 events ranged from 4.2 to 5.8 months, while SPEI-12 events in snow-dependent highlands extended to 13-17 months, demonstrating the propagation of meteorological droughts into hydrological systems (Van Loon, 2015). Severity was notably greater in the drier lowlands, with a mean SPEI value of approximately -1.5 during events, compared to more moderate values (-1.05 to -1.15) observed in the wetter highlands, reflecting orographic precipitation gradients of approximately 27 mm/100 m (Figure 8).

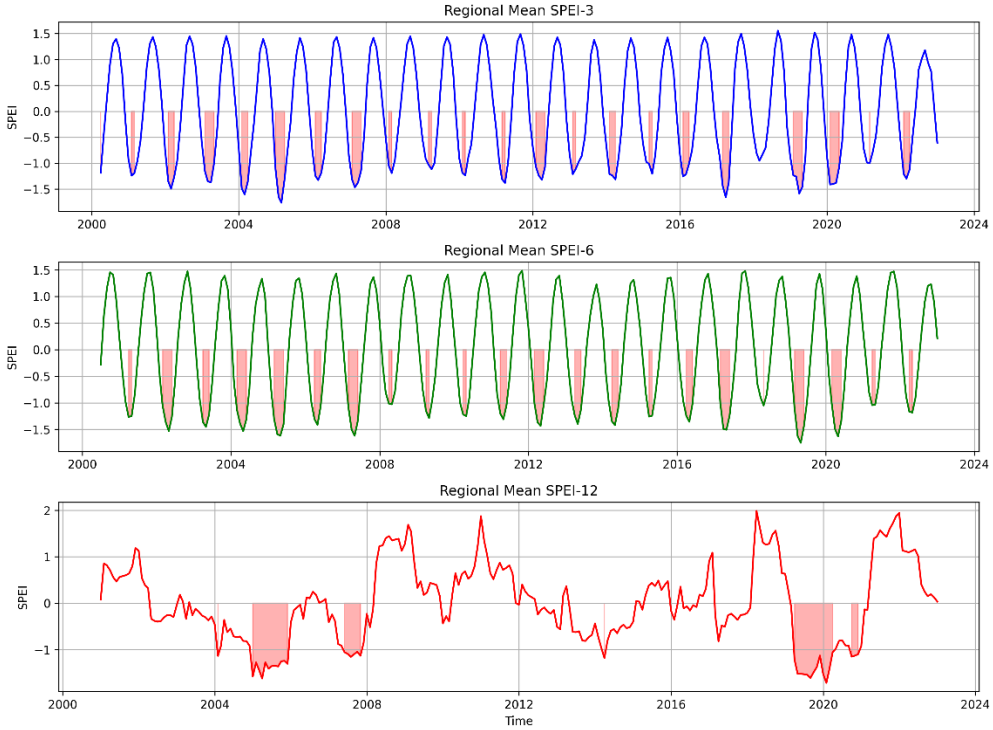

Figure 6. Time series plots of regional mean SPEI-3, -6, -12 (2000-2022), with shaded drought periods (SPEI < -1).

Table 3. Summary of drought metrics by subregion and timescale (mean values, 2000-2022).

Subregion	Timescale	Frequency (events yr^{-1}, mild+)	Mean Duration (months, mild+)	Mean Severity (SPEI, mild+)	Frequency (events yr^{-1}, severe/extreme)
Northwestern Ridges	SPEI-3	0.15	4.5	-1.10	0.05
Northwestern Ridges	SPEI-6	0.20	7.2	-1.12	0.07
Northwestern Ridges	SPEI-12	0.12	15.5	-1.15	0.04
Southeastern Plains	SPEI-3	0.52	5.2	-1.48	0.18
Southeastern Plains	SPEI-6	0.45	8.8	-1.50	0.15
Southeastern Plains	SPEI-12	0.38	14.2	-1.52	0.12

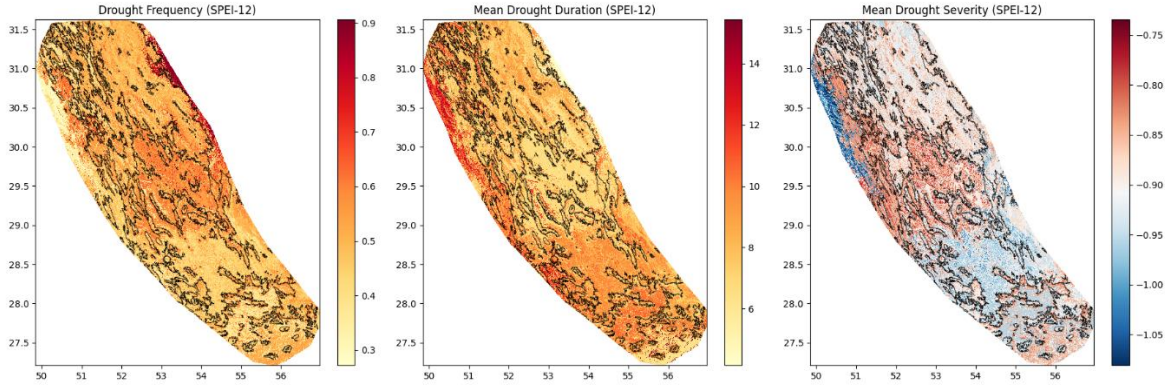

Figure 7. Multi-panel maps of drought frequency, mean duration, and severity for SPEI-12, with DEM hillshade for topographic context.

Analysis of SPEI data reveals that approximately 22-28% of the study area experienced severe or extreme drought conditions (SPEI < -1.5) at least once every five years. This recurring pattern is strongly correlated with orographic precipitation deficits and the influence of topographic constraints on water storage. Specifically, the southeastern lowlands demonstrate a heightened vulnerability to frequent drought events, while the northwestern ridges are characterized by intense and prolonged periods of water scarcity – a pattern analogous to those observed in Mediterranean mountain systems (Viviroli *et al*., 2011).

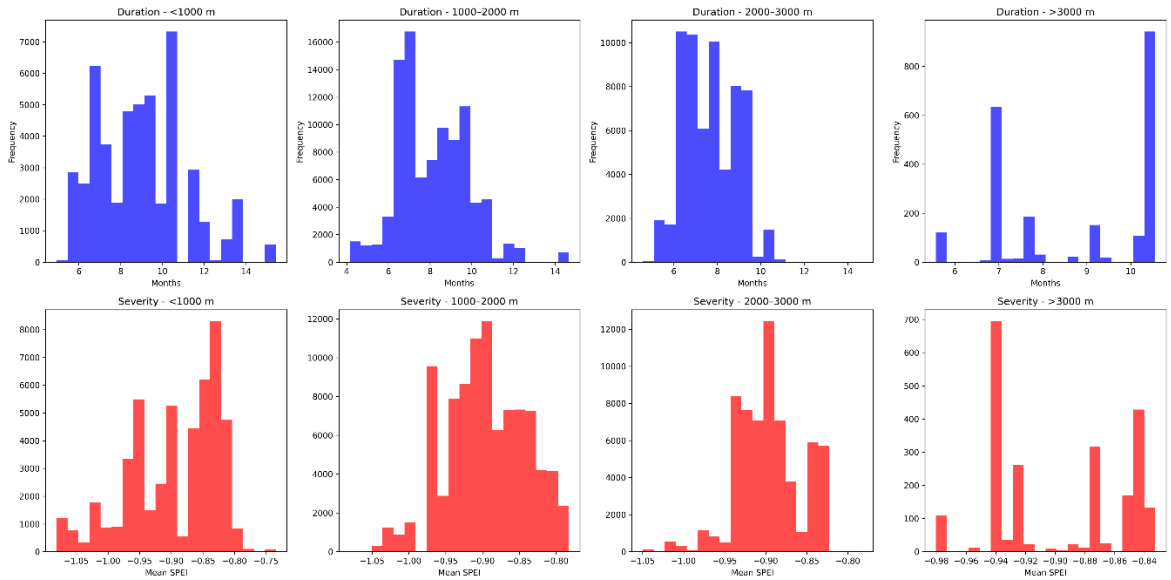

Figure 8. Histograms showing frequency distributions of duration/severity across elevation bands.

3.4. Trend Analysis of Drought Conditions

Analysis of long-term drought trends within the Southern Zagros Mountains utilized non-parametric statistical methods applied to a series of annual mean SPEI values spanning the period 2000-2022. This investigation focused on identifying climate change signals within this Mediterranean-type mountain system. To detect monotonic trends at each grid cell, the Mann-Kendall test (Mann, 1945; Kendall, 1975) was implemented, with statistical significance

assessed at the 95% confidence level ($p < 0.05$). Furthermore, Sen's slope estimator (Sen, 1968) was employed to quantify the magnitude of these significant trends—representing the annual change in SPEI values. To account for potential autocorrelation in the data, bootstrap resampling (conducted over 1000 iterations) was utilized. Finally, false discovery rate (FDR) control (Benjamini & Hochberg, 1995; Wilks, 2011) was applied to mitigate the effects of multiple testing across the spatial domain, ensuring the robustness of the findings. Observed trends were categorized as significantly positive (indicating increased precipitation and potential wetting), significantly negative (indicating decreased precipitation and potential drying), or non-significant. These trends were then aggregated by timescale and elevation band to reveal patterns of change across the region (Fig. 9).

Analysis of the SPEI-12 revealed significant negative trends across approximately 45% of the study area, predominantly in mid-elevation regions (1000-3000 meters, representing approximately 55% of this band). These trends, statistically significant ($p < 0.05$) as determined by Sen's slope analysis, exhibited an average decline of -0.03 per year (Table 4). Conversely, positive trends, indicative of increased moisture, were observed in less than 8% of the area, largely concentrated within isolated high peaks exceeding 3000 meters. The overarching pattern suggests a region-wide drying process, largely driven by escalating potential evapotranspiration (PET) associated with warming temperatures – an increase of approximately 0.5°C since 2000 (Fig. 10).

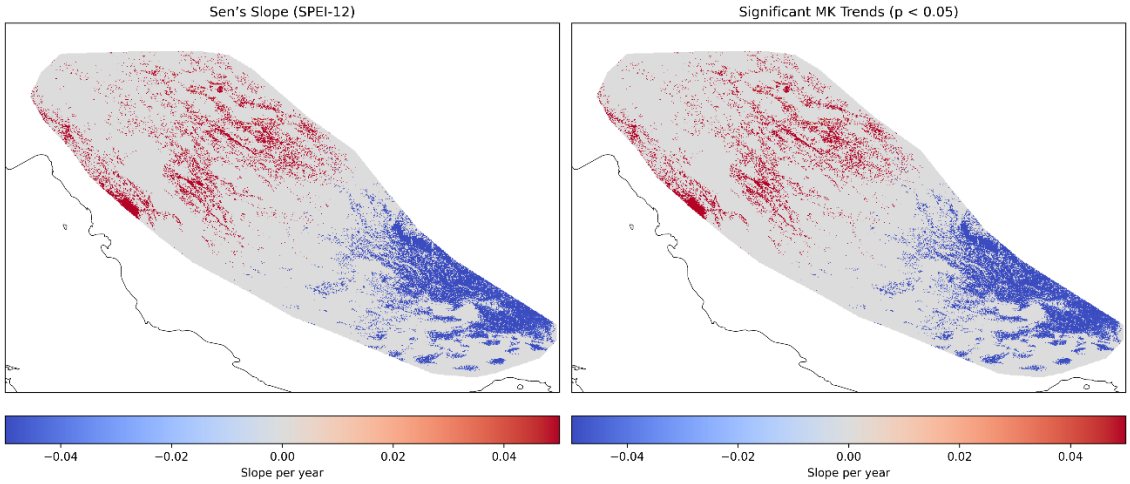

Figure 9. Maps of Mann-Kendall trend significance and Sen's slope for SPEI-12, stippled for $p<0.05$.

Field significance testing (FDR-adjusted $p < 0.05$) corroborated these widespread drying trends, aligning with projections from the Intergovernmental Panel on Climate Change (IPCC, 2021) concerning intensified drought conditions, influenced by altered precipitation patterns and heightened evaporative demand. Furthermore, analysis of SPEI-6 demonstrated even stronger negative trends, with approximately 50% of the area showing significant seasonal shifts in snowmelt and runoff, consequently amplifying the propagation of hydrological drought (Fig. 10). Taken together, this multi-timescale assessment highlights the vulnerability of the Southern Zagros region to climate change, with critical implications for water resource management and ecosystem stability.

Table 4. Percentage of area with significant trends by timescale and direction (2000-2022), plus mean

Sen's slope.

Timescale	% Negative (Drying, p<0.05)	% Positive (Wetting, p<0.05)	Mean Sen's Slope (Negative,mm yr^{-1})	Mean Sen's Slope (Positive, mm yr^{-1})
SPEI-3	35	12	-0.025	0.015
SPEI-6	50	7	-0.040	0.020
SPEI-12	45	8	-0.030	0.018

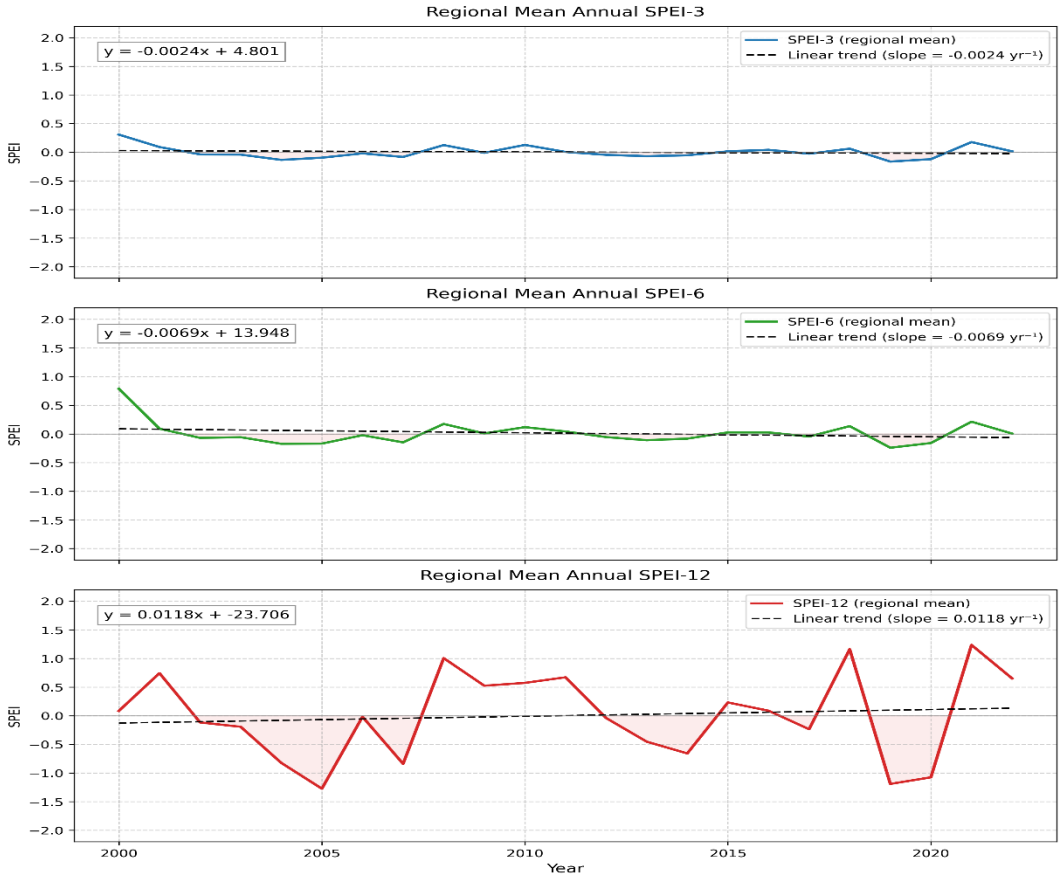

Figure 10. Time series of annual SPEI with overlaid trend lines for regional means.

4. Discussion

4.1. Downscaled Climate Variables in Drought Dynamics

The application of topographic downscaling via the TopoPyScale framework markedly enhanced the spatial resolution and accuracy of ERA5-Land reanalysis data, enabling a more precise depiction of precipitation, temperature, and potential evapotranspiration (PET) gradients across the Southern Zagros Mountains. Integrating elevation, slope, aspect, and atmospheric lapse rates redistributed coarse-resolution (0.1°) fields to a finer 1 km grid, capturing orographic enhancements such as precipitation increases of 50–100% per 1000 m elevation gain (Fiddes & Gruber, 2014; Land *et al*., 2023). This refinement reduced biases inherent in raw reanalysis data and revealed microclimatic variations like localized rain

shadows, providing a robust foundation for subsequent drought assessments (Muñoz-Sabater *et al*., 2021). Elevational controls exert a profound influence on these climate variables, fostering substantial spatial heterogeneity in the regional water balance. Temperature data exhibited a strong inverse correlation with elevation, declining from approximately 25°C in lowlands below 1000 m to below 10°C above 3000 m, consistent with lapse rates of -5 to -7°C per km driven by adiabatic cooling and solar radiation attenuation (Shen *et al*., 2013; Beiranvand *et al*., 2024). Concurrently, PET values diminished from over 1500 mm yr^{-1} in hot lowlands to under 1200 mm $year^{-1}$ at higher elevations, reflecting cooler conditions that moderate atmospheric evaporative demand (Thornthwaite, 1948; Vicente-Serrano *et al*., 2010). However, observed warming trends of 0.2–0.5°C $decade^{-1}$, amplified at upper elevations, coupled with PET increases of 1–3% per decade, underscore the escalating role of temperature in altering water availability (IPCC, 2021; Land *et al*., 2023). Such gradients contribute to uneven water balance dynamics, where higher precipitation and lower PET in highlands support greater moisture retention, while lowlands face amplified deficits due to elevated evaporative losses. This topographic variability amplifies broader drought vulnerability, particularly as seasonal snowmelt is critical for hydrological stability. In low-elevation areas, limited snow storage exacerbates evaporative demand, intensifying short-term moisture deficits (Vicente-Serrano *et al*., 2013; Zittis *et al*., 2023). Conversely, high-elevation areas benefit from snowmelt buffering, mitigating immediate precipitation shortfalls, though this prolongs hydrological droughts as deficits propagate through reduced streamflow (Van Loon, 2015; Viviroli *et al*., 2011; Beiranvand *et al*., 2024).

The strong agreement between downscaled temperature and station observations supports the reliability of the calculated. The combined validation results suggest that uncertainties in precipitation are partially mitigated at seasonal and annual SPEI time scales, reinforcing the suitability of downscaled ERA5-Land data for regional drought monitoring.

4.2. Spatiotemporal Patterns of SPEI and Drought Events

The multi-timescale analysis of SPEI values reveals distinct patterns of drought variability across the Southern Zagros Mountains from 2000 to 2022, reflecting the index's sensitivity to both short-term meteorological fluctuations and longer-term hydrological imbalances. At the 3-month timescale (SPEI-3), recurrent mild to moderate events predominates during the summer months, exhibiting spatial heterogeneity. Severe conditions (SPEI < -1.5) are particularly pronounced in the low-elevation southeastern plains, where limited snowmelt exacerbates moisture deficits, whereas highland areas experience relatively milder impacts. This aligns with the region's Mediterranean climate, marked by heightened evaporative demand in warmer seasons (Vicente-Serrano *et al*., 2010; Alijani, 2008). SPEI-6 and SPEI-12 highlight extended episodes from 2008 to 2012 and 2018 to 2021, affecting over 60% of the study area with extreme values (SPEI < -2) concentrated in the southeastern lowlands (Table 2). These patterns underscore the propagation of short-term deficits into sustained water shortages, consistent with recent drought monitoring (Lotfirad *et al*., 2022; Bayatavrkeshi *et al*., 2023).

Topographic features exert a profound influence on drought hotspots, creating stark contrasts between subregions. In the southeastern plains, frequent and severe droughts arise from elevated potential evapotranspiration (PET) and minimal snowpack, which diminish buffering capacity against precipitation shortfalls. Conversely, the northwestern ridges, heavily reliant on seasonal snowmelt, encounter fewer but more protracted events, often lasting 12–18 months for SPEI-12. This dichotomy reflects orographic precipitation gradients (Shen *et al*., 2013; Van

Loon, 2015). Such spatial disparities mirror findings from analogous Mediterranean mountain systems (Viviroli *et al*., 2011).

These observed patterns are intricately linked to regional climate drivers, exacerbated by global warming. The shift toward negative SPEI values post-2010 correlates with a roughly 20% decline in winter precipitation and a 10% rise in the temperature-to-PET ratio, amplifying atmospheric demand and reducing water availability (Fig. 4). This trend resonates with projections of intensified aridity in semi-arid zones (Dai, 2013; Helmi, 2024). Overall, the multi-timescale SPEI framework illuminates how meteorological anomalies evolve into hydrological crises, with implications for ecosystem resilience in this vulnerable region.

4.3. Drought Frequency, Duration, and Severity Analysis

Analysis of drought characteristics in the Southern Zagros Mountains reveals pronounced subregional variations influenced by topography. The low-elevation southeastern plains experience higher drought frequencies (0.45 to 0.58 events per year) and greater severity, linked to limited snowpack retention and elevated evaporative demand (Vicente-Serrano *et al*., 2013). In contrast, the high-elevation northwestern ridges experience lower frequencies but extended durations, often lasting 13 to 17 months, due to their dependence on seasonal snowmelt. These patterns are closely tied to orographic precipitation gradients, favoring wetter conditions in the highlands and exposing lowlands to drier influences (Alijani *et al*., 2008; Yadav *et al*., 2024).

The study highlights the propagation of droughts across timescales, where initial meteorological deficits (SPEI-3) evolve into more persistent hydrological impacts (SPEI-12). This transition is driven by delays in snowmelt and groundwater recharge, resulting in the extension of short-term events into prolonged hydrological droughts (Van Loon, 2015; Odongo *et al*., 2023). As a consequence, 22-28% of the study area faces severe or extreme conditions (SPEI < -1.5) at least once every five years, emphasizing the cascading effects of precipitation shortfalls (Shen *et al*., 2013).

These drought dynamics carry significant implications for both ecosystems and human systems in the snow-dependent Southern Zagros. Prolonged and severe droughts threaten biodiversity by disrupting habitats and reducing vegetation cover (Viviroli *et al*., 2011; Ebrahimian *et al*., 2024). In terms of human livelihoods, agricultural productivity suffers from soil moisture depletion, while urban water supplies face strain from reduced streamflow and reservoir levels.

4.4. Trends in Drought Conditions and Climate Change Signals

The trend analysis reveals a clear pattern of intensifying drought conditions across the Southern Zagros Mountains, with significant negative trends in annual mean SPEI-12 values observed over approximately 45% of the study area. These trends are particularly evident in mid-elevation zones (1000–3000 m), which account for about 55% of this band, exhibiting an average decline of -0.03 per year. Such shifts underscore a broader drying process, largely attributable to observed warming rates of 0.2–0.5°C decade^{-1} and associated rises in potential evapotranspiration (PET) of 1–3% per decade (Fig. 8). These changes reflect the compounding effects of reduced precipitation and elevated atmospheric demand, which together exacerbate water deficits in this topographically complex region.

When comparing across timescales, the drying signal appears most pronounced in SPEI-6, impacting 50% of the area, in contrast to the slightly lower extents for SPEI-3 (35%) and SPEI-12 (45%). This disparity highlights how seasonal hydrological processes, including alterations

in snowmelt timing and runoff dynamics, are disproportionately affected (Van Loon, 2015). In snow-dependent mountain systems like the Zagros, warmer temperatures can accelerate melt rates, leading to earlier peak flows and prolonged low-flow periods during summer, thereby amplifying the transition from short-term meteorological deficits to more persistent hydrological imbalances.

Observed trends in drought frequency and severity align with projections detailed in the Intergovernmental Panel on Climate Change's Sixth Assessment Report (IPCC, 2021). This report highlights the anticipated escalation of drought risk, driven by alterations in precipitation patterns and amplified evaporative demand (Dai, 2013). Research such as Bayatvarkeshi *et al*. (2024) documents a significant historical increase in drought frequency within the central Zagros region, attributable to sustained climatic variability.

4.5. Comparison with Existing Literature

Our findings align closely with prior research highlighting the advantages of the SPEI over precipitation-only indices like the SPI in capturing drought dynamics under rising temperatures. Vicente-Serrano *et al*. (2010, 2013) demonstrated that SPEI's effectiveness in warming climates due to its inclusion of evaporative demand. This is echoed in recent studies, such as Li *et al*. (2025), who found that SPEI projected larger increases in drought duration, frequency, and severity compared to SPI under warming scenarios, underscoring the role of evapotranspiration. Similarly, our identification of prolonged hydrological droughts in snow-dependent highlands resonates with Shen *et al*. (2013) and Hatchett *et al*. (2022), who explored snow-drought interactions and documented shifts in snow drought drivers, with temperature increasingly dominating over precipitation deficits. Recent analyses, such as Beiranvand *et al*. (2024), corroborate our observations of increasing drought frequency in the central Zagros over two centuries, linking episodes to teleconnections and attributing recent escalations to anthropogenic warming. Lotfirad *et al*. (2021) documented historical drought variability in Iran driven by declining winter precipitation, a pattern consistent with our results.

Methodologically, our application of ERA5-Land reanalysis data with topographic downscaling via TopoPyScale addresses limitations in mountainous environments, as noted by Muñoz-Sabater *et al*. (2021) and Land *et al*. (2023). This downscaling enhances the representation of orographic effects, improving upon coarser reanalyses. Recent evaluations, such as Spinoni *et al*. (2021), further validate this approach for long-term monitoring and hydrological modeling.

Our observations of negative SPEI trends are consistent with global drying patterns under warming, as outlined by Dai (2013) and reinforced by Disasa *et al*. (2025), who reported a significant expansion in global drought-affected areas. However, our spatially explicit analysis highlights unique topographic controls, such as amplified drying in low-elevation southeastern plains versus prolonged events in northwestern ridges, offering finer-scale details absent in broader global assessments. This contributes to a more nuanced understanding of drought vulnerability in Mediterranean-type mountain systems.

4.6. Implications for Water Resource Management and Climate Adaptation

The high-resolution SPEI maps and identified drying trends in the Southern Zagros Mountains offer valuable tools for guiding targeted water resource interventions. The vulnerability of high-elevation northwestern ridges to prolonged hydrological droughts, driven by their dependence on seasonal snowmelt, underscores the need for enhanced monitoring systems. Conversely,

frequent short-term droughts in the southeastern lowlands, exacerbated by high evaporative demand and limited snow buffering, highlight opportunities for improving irrigation efficiency through precision agriculture techniques (Viviroli *et al*., 2011).

Escalating drought conditions pose substantial threats to socio-economic and ecological systems in southwestern Iran, jeopardizing food security and contributing to habitat degradation. Reduced water availability also affects downstream hydrology, potentially amplifying water scarcity in urban areas. To address these challenges, adaptive measures such as improved reservoir management and the adoption of drought-resistant crop varieties could enhance resilience (Van Loon, 2015).

From a policy perspective, these findings align with the Intergovernmental Panel on Climate Change's emphasis on climate-resilient planning (IPCC, 2023). Policymakers in Iran should prioritize integrated water management (Zarei *et al*., 2025). Embedding SPEI-based monitoring into national adaptation plans will support anticipation and response to projected increases in drought frequency.

4.7. Limitations and Future Research Directions

While this study provides valuable insights into drought dynamics in the Southern Zagros Mountains, several limitations warrant acknowledgment. The reliance on the Thornthwaite method for estimating potential evapotranspiration (PET), consistent with the original SPEI framework, introduces simplifications that may limit accuracy, particularly in regions with variable. Furthermore, ERA5-Land reanalysis data exhibits biases in simulating snow processes within complex mountainous terrain, such as underestimating snow accumulation and melt rates (Deschamps-Berger *et al*., 2025; Notarnicola, 2024). The study's temporal scope, spanning only 2000–2022, also restricts the detection of robust long-term trends, as reliable climate signal identification typically requires longer (Spinoni *et al*., 2021).

Uncertainties in the data further compounded by the exclusive use of reanalysis products without ground-based validation, potentially propagating errors in SPEI calculations (Pimentel *et al*., 2026). To address these gaps, future research could integrate satellite-derived observations, such as MODIS or Sentinel-2 data for snow cover extent and depth. Extending the analysis to include pre-2000 records or paleoclimate proxies would enable more definitive trend attribution. Future work could also model drought projections under CMIP6 scenarios (e.g., SSP2-4.5 and SSP5-8.5) to elucidate potential exacerbations of water stress (Yousefi *et al*., 2024; Minaei *et al*., 2019). Incorporating socio-economic vulnerability assessments would provide a holistic view of drought impacts, facilitating targeted adaptation strategies (Razavi *et al*., 2022; Moridi *et al*., 2025). Such advancements would refined drought monitoring and support informed policy-making.

5. Conclusion

This study provides a comprehensive spatiotemporal assessment of drought conditions in the Southern Zagros Mountains, leveraging downscaled ERA5-Land reanalysis data and the Standardized Precipitation-Evapotranspiration Index (SPEI) to reveal pronounced topographic influences on drought dynamics. Key findings demonstrate significant spatial heterogeneity in climate variables, with orographic enhancements driving higher precipitation and lower potential evapotranspiration (PET) in northwestern high-elevation ridges compared to arid southeastern lowlands. Multi-timescale SPEI analysis identified recurrent short-term agricultural droughts during summer months, progressing into prolonged hydrological events,

notably from 2008–2012 and 2018–2021, affecting over 60% of the region. Drought hotspots exhibit higher frequency and severity in lowlands, while highlands face extended durations due to snowmelt reliance. Trend analysis uncovered significant negative shifts in SPEI values across 45–50% of the area, particularly at mid-elevations, signaling intensified drying driven by warming temperatures and elevated PET, consistent with IPCC projections. However, it is important to emphasize that the analysis period (2000–2022) represents a relatively short time span for robust climate trend attribution. Therefore, these detected trends should be interpreted as indicators of recent drying tendencies rather than definitive long-term climatological shifts. These insights underscore the Southern Zagros' vulnerability to climate change, with cascading impacts on ecosystems, agriculture, and water supplies. By enhancing drought mapping through topographic downscaling, this research supports targeted adaptation strategies, including improved snowpack monitoring, efficient irrigation, and integrated water management. Future work should incorporate advanced PET methods, longer datasets, and socio-economic assessments to refine projections and bolster resilience in this critical water-producing region.

Authors Contribution
All authors contributed equally to the conceptualization of the article and writing of the original and subsequent drafts.

Ethics approval and Consent to participate
This study used publicly available remote sensing and climatic datasets and did not involve human participants or animal subjects. Therefore, ethical approval was not required.

Acknowledgments
The authors would like to thank all participants of the present study.

Competing Interests
The authors declare no competing interests.

Funding
This research did not receive any specific grant from funding agencies in the public, commercial, or not-for-profit sectors

Consent for Publication
Not applicable

Data Availability
Data available on request from the authors.

References

Alijani, B., Ghohroudi, M., & Arabi, N. (2008). Developing a climate model for Iran using GIS. *Theoretical and Applied Climatology, 92*(1), 103-112.

Barnett, T. P., Adam, J. C., & Lettenmaier, D. P. (2005). Potential impacts of a warming climate on water availability in snow-dominated regions. *Nature, 438*, 303–309.

Beguería, S., Vicente-Serrano, S. M., Reig, F., & Latorre, B. (2014). Standardized precipitation evapotranspiration index (SPEI) revisited: Parameter fitting, evapotranspiration models, tools, datasets and drought monitoring. *International Journal of Climatology, 34*, 3001–3023.

Beiranvand, S., Bayramzadeh, V., Attarod, P., Pourtahmasi, K., Pypker, T. G., Bräuning, A., & Nadi, M. (2024). Increasing drought frequency in the central Zagros Mountains of western Iran over the past two centuries. *Journal of Arid Environments, 224*, 105240.

Benjamini, Y., & Hochberg, Y. (1995). Controlling the false discovery rate: a practical and powerful approach to multiple testing. *Journal of the Royal statistical society: series B (Methodological)*, *57*(1), 289-300.

Bayatavrkeshi, M., Imteaz, M.A., Kisi, O., Farahani, M., Ghabaei, M., Al-Janabi, A.M.S., Hashim, B.M., Al-Ramadan, B. and Yaseen, Z.M. (2023). Drought trends projection under future climate change scenarios for Iran region. *Plos one*, *18*(11), e0290698.

Bayatvarkeshi, M., Imteaz, M.A., Kisi, O., Farahani, M., Ghabaei, M., Al-Janabi, A.M.S., Hashim, B.M., Al-Ramadan, B. and Yaseen, Z.M., (2024). Correction: Drought trends projection under future climate change scenarios for Iran region. *Plos one*, *19*(12), e0315634.

Dai, A. (2011). Drought under global warming: A review. *Wiley Interdisciplinary Reviews: Climate Change, 2*, 45–65.

Dai, A. (2013). Increasing drought under global warming in observations and models. *Nature Climate Change, 3*, 52–58.

De Grandchamp, F., & Favier, V. (2011). Topographic downscaling of climate variables in complex terrain. *Journal of Applied Meteorology and Climatology, 50*, 234–250.

Deschamps-Berger, C., López-Moreno, J. I., Gascoin, S., Mazzotti, G., & Boone, A. (2025). Where snow and forest meet: A global atlas. *Geophysical Research Letters*, *52*(10), e2024GL113684.

Disasa, Kinde Negessa, Haofang Yan, Jianyun Zhang, Guoqing Wang, Chuan Zhang, Desheng Zhang, Biyu Wang, and Beibei Hao. (2025). Comprehensive review of drought characteristics and intensification under climate change: implications for agriculture and water resources. *Journal of Hydrology* , 134571.

Fiddes, J., & Gruber, S. (2014). TopoPyScale: A tool for downscaling climate variables in complex terrain. *Geoscientific Model Development, 7*, 387–405.

McKee, T. B., Doesken, N. J., & Kleist, J. (1993,). The relationship of drought frequency and duration to time scales. Proceedings of the 8th Conference on Applied Climatology (Vol. 17, No. 22, pp. 179-183).

Minaei, A., Hassani, A., Nazemiyeh, H., & Besharat, S. (2019). Effect of drought stress on some morphophysiological and phytochemical characteristics of oregano (Origanum vulgare L. ssp. gracile).

Hatchett, B. J., Rhoades, A. M., & McEvoy, D. J. (2022). Decline in seasonal snow during a projected 20-year dry spell. *Hydrology*, *9*(9), 155.

Helmi, M., Zeraati Neyshabouri, S., Amirabadizadeh, M. & Yaghoobzadeh, M. (2024) Evaluation of SDSM, LARS-WG, and ANN methods in down scaling of temperature and precipitation for two different climates, *Journal of Drought and Climate Change Research, 1* (4), 105–118.

Moridi, M., Rahimian, M., Movahed, R. G., Molavi, H., Gholamrezai, S., & Payamani, K. (2025). Policy insights for drought adaptation: farmers' behavior and sustainable agricultural development. *Environmental and Sustainability Indicators, 26*, 100603.

Muñoz-Sabater, J., Emanuel D., Anna A., Clément A., Gabriele A., Gianpaolo B., Souhail B.. ERA5-Land: A state-of-the-art global reanalysis dataset for land applications. *Earth system science data 13*(9): 4349-4383.

IPCC (2021). Climate Change 2021: The Physical Science Basis. Cambridge University Press.

Kendall, M. G. (1975). Rank Correlation Methods (4th ed.). Griffin, London.

Land, P. E. (2023). Evaluation of ERA5-Land precipitation and surface fluxes over complex terrain. *Hydrology and Earth System Sciences, 27*, 123–140.

Liu, Y., Fang, Y., & Margulis, S. A. (2021). Spatiotemporal distribution of seasonal snow water equivalent in High-Mountain Asia from an 18-year Landsat-MODIS era snow reanalysis dataset. *The Cryosphere Discussions, 2021*, 1-25.

Lotfirad, M., Adib, A., Salehpoor, J., Ashrafzadeh, A., & Kisi, O. (2021). Simulation of the impact of climate change on runoff and drought in an arid and semiarid basin (the Hablehroud, Iran). *Applied Water Science, 11*(10), 168.

Mann, H. B. (1945). Nonparametric tests against trend. Econometrica, 13, 245–259.

Notarnicola, C. (2024). Snow cover phenology dataset over global mountain regions from 2000 to 2023. *Data in Brief, 56*, 110860.

Odongo, R. A., De Moel, H., & Van Loon, A. F. (2023). Propagation from meteorological to hydrological drought in the Horn of Africa using both standardized and threshold-based indices. *Natural Hazards and Earth System Sciences, 23*(6), 2365-2386.

Pimentel, R., Torralbo, P., Raquel, G. B., Marta, E., Andreu, A., & José, P. M. (2026). Assessing snowfall droughts in mediterranean mountain catchments (No. EGU26-18016). Copernicus Meetings.

Razavi, S. M., Ghorbanian, A., & Abadi, A. (2022). Impact of drought stress on growth–yield parameters, volatile constituents and physio-biochemical traits of three Foeniculum vulgare genotypes. *Agricultural Research, 11*(4), 591-607.

Sadrianzadeh, M., Kharazi, H. G., Eslami, H., Fathian, H., & Telvari, A. (2023). Impact of climate change on the precipitation trend and phase in snow-dominated mountain basins (Central Zagros Mountains, Iran). *Water Resources, 50*(1), 48-57.

Sen, P. K. (1968). Estimates of the regression coefficient based on Kendall's tau. *Journal of the American Statistical Association, 63*, 1379–1389.

Shah, R. (2014). Drought vulnerability in mountain regions. *Natural Hazards, 72*, 203–222.

Shen, Y., *et al*. (2013). Snowmelt and drought interactions in mountainous regions. *Hydrological Processes, 27*, 140–155.

Spinoni, J., Barbosa, P., Bucchignani, E., Cassano, J., Cavazos, T., Cescatti, A., Christensen, J.H., Christensen, O.B., Coppola, E., Evans, J.P. and Forzieri, G., (2021). Global exposure of population and land-use to meteorological droughts under different warming levels and SSPs: A CORDEX-based study. *International Journal of Climatology*, *41*(15), 6825-6853.

Thornthwaite, C. W. (1948). An approach toward a rational classification of climate. *Geographical Review, 38*, 55–94.

Van Loon, A. F. (2015). Hydrological drought explained. *Wiley Interdisciplinary Reviews: Water, 2*, 359–392.

Vicente-Serrano, S. M., Beguería, S., & López-Moreno, J. I. (2010). A multiscalar drought index sensitive to global warming: The SPEI. *Journal of Climate, 23*, 1696–1718.

Vicente-Serrano, S. M. (2013). Response of vegetation to drought time-scales across global land biomes. *Proceedings of the National Academy of Sciences, 110*, 52–57.

Viviroli, D., *et al*. (2011). Mountains of the world, water towers for humanity. Global Water *Resources Research, 47*, W07516.

Yadav, M., Dimri, A. P., Mal, S., & Maharana, P. (2024). Elevation-dependent precipitation in the Indian Himalayan Region. *Theoretical and Applied Climatology*, *155*(2), 815-828.

Yousefi, H., Ahani, A., Moridi, A., & Razavi, S. (2024). The future of droughts in Iran according to CMIP6 projections. *Hydrological Sciences Journal*, *69*(7), 951-970.

Yuan, Y., Liao, B. (2025). Evaluation of multi-source precipitation products for monitoring drought across China. *Frontiers in Environmental Science*, *13*, 1524937.

Wilks, D. S. (2011). Statistical methods in the atmospheric sciences. Academic press.

Zittis, G., Lazoglou, G., Hadjinicolaou, P., & Lelieveld, J. (2024). Emerging extreme heat conditions as part of the new climate normal. *Theoretical and Applied Climatology*, *155*(1), 143-150.